

Relationship between Rubisco activase isoform levels and photosynthetic rate in different leaf positions of rice plant

D. WANG^{*}, Q. LU^{*}, X.F. LI^{*}, Q. S. JIANG^{*}, J.X. WU^{**},^{***}, and D.A. JIANG^{*,+}

State Key Laboratory of Plant Physiology and Biochemistry, College of Life Sciences, Zhejiang University, Hangzhou 310058, China
Institute of Biotechnology, Zhejiang University, Hangzhou 310029, China^{**}

Abstract

To investigate into the relationship between two Rubisco activase (RCA) isoforms and photosynthetic rate, a set of enzyme-linked immunosorbent assay (ELISA) were developed for accurate quantification of two RCA polypeptides based on two specific monoclonal antibodies against different RCA isoforms. The results showed that content of RCA small isoform (RCA_S) was 5-fold more than that of RCA large isoform (RCA_L) content in all leaves and the RCA_L/RCA_S ratio reached maximum in the leaf with the highest photosynthetic rate. Although the difference in two RCA polypeptides accumulation in leaves was caused by different transcript level of two isoforms, the decrease of RCA_L/RCA_S ratio during leaf aging was not attributed to transcriptional regulation. The leaves with higher photosynthetic capacity exhibited higher RCA_L/RCA_S ratio and the decrease in photosynthetic rate and Rubisco activation state highly correlated with the decline of RCA_L/RCA_S ratio during leaf aging. Our results suggest that there is a post-transcriptional mechanism regulating the RCA_L/RCA_S ratio, which may play as a regulator modulating photosynthetic capacity during leaf aging in rice plant.

Additional key words: ELISA, quantification, senescence, *Oryza sativa* L.

Introduction

Ribulose-1,5-bisphosphate carboxylase/oxygenase (Rubisco) is a key enzyme for photosynthesis. Before it catalyzes the carboxylation or oxygenation of ribulose-1,5-bisphosphate (RuBP), Rubisco needs to be activated by the ATP-dependent enzyme Rubisco activase (RCA) (Streusand and Portis 1987, Portis 1992, Salvucci and Ogren 1996). RCA is a nuclear-encoded enzyme, synthesized in cytosol as a precursor and processed into a mature polypeptide after it is imported into the chloroplast stroma (Portis 1990). Two mature RCA polypeptides with molecular mass ranging between 41 and 47 kDa are present in most plants (Salvucci *et al.* 1987, Werneke *et al.* 1989, Rundle and Zielinski 1991, Portis 2003). One gene encodes two RCA polypeptides of 45 kDa (RCA_L) and 41 kDa (RCA_S) arising from unique

alternative splicing of pre-mRNA in rice plant (To *et al.* 1999). Analysis of cDNA and the relevant genomic DNA sequences indicates that the two isoforms of rice RCA polypeptides are 99% identical, except for a 33 amino acids addition and a 5 amino acid substitution at the carboxyl terminus of RCA_L (To *et al.* 1999, Zhang and Komatsu 2000). Two RCA polypeptides are encoded by two separate genes and the transcription rate of the two RCA genes differed obviously during leaf development in barley leaves (Rundle and Zielinski 1991). Vargas-Suárez *et al.* (2004) reported that the accumulation of two maize RCA polypeptides, encoded by two separate genes, was regulated during leaf development. Two spinach RCA isoforms arising from alternative splicing were capable of promoting Rubisco activation, but they differed remark-

Received 11 June 2009, *accepted* 28 December 2009.

[†]Corresponding author: fax: +86-571-88206461, e-mail: dajiang@zju.edu.cn and wujx@zju.edu.cn

Abbreviations: BSA – bovine serum albumin; C_i – intercellular CO_2 concentration; ELISA – enzyme-linked immunosorbent assay; g_s – stomatal conductance; HRP – Horseradish peroxidase; IPTG – isopropylthio- β -D-thiogalactoside; mAbs – monoclonal antibodies; PBS – phosphate buffered saline; PBST – PBS containing 0.05% Tween 20; PFD – photon flux density; PMSF – phenylmethylsulfonyl fluoride; P_N – net photosynthetic rate; PVP – polyvinylpyrrolidone; Rubisco – ribulose-1,5-bisphosphate carboxylase/oxygenase; RCA – Rubisco activase; RCA_L – RCA large isoform; RCA_S – RCA small isoform; RLS – Rubisco large subunit; RSS – Rubisco small subunit.

Acknowledgments: This work was financially supported by the National Natural Science Foundation (30971703, 30771302 and 30471051).

ably in enzyme activity (Shen *et al.* 1991). The activity of RCA_L was regulated by redox state *via* thioredoxin- β (Zhang and Portis 1999, Zhang *et al.* 2002), and this redox regulation was due to an interaction between carboxyl extension and nucleotide-binding pocket in RCA_L (Wang and Portis 2006). Although rice leaves accumulate more RCA_S than RCA_L (To *et al.* 1999), it still keeps unknown whether or not the two isoforms change in leaf development and what relationship is between them and photosynthetic capacity.

In this work, we first set an ELISA method for

Materials and methods

Preparation of antigen and production of monoclonal antibodies: The common protein fragment of RCA_L and RCA_S (named as RCA-COM) and the specific segment located at the C-terminus of the RCA_L (named as RCA-END) were expressed separately in *E. coli* using a T7 expression system according to the manufacturer's instructions (Novagen, Madison, WI, USA). For RCA-COM , a 1284-bp-common DNA fragment was amplified by PCR from full length of rice RCA gene using a forward primer 5'-TAGAATTCTCCACTCCGACCA ACTTC-3', containing an *Eco*RI site, and a reverse primer 5'-CACAAAGCTTCACAAGCATGTATCCG TAG-3', containing a *Hind* III site. For RCA-END , a 114 bp DNA fragment which encoded the specific 38 amino acids located at the C-terminus of the RCA_L was amplified by PCR from full length of rice RCA gene using a forward primer 5'-CGGAATTCCAAGGAGC ACAGCAAGCAG-3', containing an *Eco*RI site, and a reverse primer 5'-TCTAACGCTTAAAGGTGTAAAGGC AGCTG-3', containing a *Hind* III site. The amplified fragments were digested with *Eco*RI and *Hind* III, and then subcloned into the expression vector pET-28a or pET-32a (Novagen, Madison, WI, USA) respectively, to produce two His-tag fusion proteins: RCA-COM and RCA-END (Fig. 1). After transformation into *E. coli* BL21 (DE3) cells, production of the fusion protein was directed by T7 polymerase, which was induced by 1 mM isopropylthio- β -D-thiogalactoside (IPTG) for 6 h. The

quantitative analysis of two RCA isoforms and Rubisco subunits based on specific monoclonal antibodies (mAbs). Then, we investigated the dynamic expression of two RCA isoforms in mRNA level and protein level, net photosynthetic rate (P_N) and Rubisco activation in different leaf positions. Based on the results of these experiments, we provide details about the regulation of two RCA isoform proteins and the relationship between accumulation of two RCA isoforms and photosynthetic capacity during leaf aging in rice plants.

recombinant 6×His-tagged pET-28a-COM and pET-32a-END protein were purified over Ni^{2+} -nitrilotriacetic acid affinity columns under denaturing conditions, as instructed by the manufacturer (Qiagen, Hilden, Germany). The expressed fusion proteins were checked by SDS-PAGE and Western analysis performed as described previously (Lu *et al.* 2008).

Rubisco purification was performed by the method of Makino *et al.* (1983). The purified fusion RCA proteins and purified Rubisco were used as an antigen to produce specific monoclonal antibodies by the method of Zhou *et al.* (2005).

Horseradish peroxidase (HRP)-conjugated antibodies: MAbs were conjugated to HRP (Sigma, RZ>3), respectively, by the periodate method of Wilson and Nakane (1978). The horseradish peroxidase-conjugated mAbs were stored at 4°C in 50 mM Tris (pH 8.0), 40% glycerol, 0.1% NaN_3 , and 1% bovine serum albumin (BSA).

Rubisco and RCA protein quantification by ELISA: About 6–7 cm^2 (0.1 g) of frozen rice leaves were ground to a powder using mortar and pestle with liquid N_2 , a small amount of quartz sand and insoluble polyvinyl-polypyrrolidone (PVP), then homogenized with 2 ml cooled cover buffer at 0–4°C. The cover buffer contains 50 mM carbonate/bicarbonate buffer (pH 9.6), 2 mM MgCl_2 , 1 mM EDTA, 0.4 mM ATP, 1 mM phenyl-

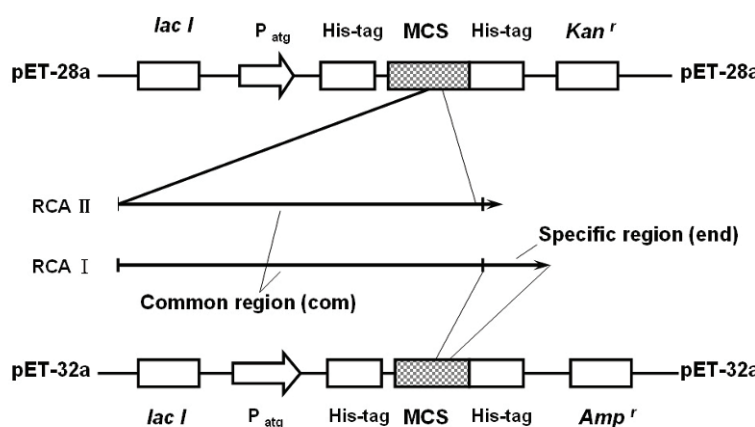


Fig. 1. Schematic structure of recombinant plasmids pET-28a-COM and pET-32a-END. A 1284 bp DNA fragment encoding the common region of RCA_L and RCA_S , and a 114 bp DNA fragment encoding the specific region of RCA_L were cloned into *E. coli* expression vector pET-28a or pET-32a, respectively.

methylsulfonyl fluoride (PMSF), 2 mM benzamidine, and 0.01 mM leupetine. The homogenate was centrifuged at 15×000 g for 10 min at 4°C. The supernatant was used to determine the concentration of Rubisco and RCA protein.

A set of ELISA measurements for quantitative analysis of Rubisco subunits and two activase isoforms were developed based on the methods of Demirevska-Kepova (1990). In brief, flat-bottom immunoassay polystyrene microplates (Costar, NY, USA) were used. Microtiter plate was coated with 100 μ l of diluted sample supernatant. In control wells, 3% (w/v) BSA was used instead of sample. The plates were incubated at 37°C for 2 h and washed three times with PBS (136.7 mM NaCl, 2.68 mM KCl, 1.47 mM KH₂PO₄, 8.38 mM Na₂HPO₄ · 12 H₂O, 0.05% Tween 20, pH 7.4). The plates were then incubated in 3% (w/v) BSA in PBS (200 μ l per well) for 0.5 h at 37°C, and they were washed three times with PBS. Horseradish peroxidase-conjugated monoclonal antibodies (diluted in PBS containing 3% BSA; 100 μ l per well) against the Rubisco large subunit, Rubisco small subunit, RCA or RCA_L from rice were added and incubated for 1 h at 37°C. After washing the plates five times with PBS containing 0.05% Tween 20 (PBST), 100 μ l of substrate solution (0.1 M citric acid, 0.2 M Na₂HPO₄ · 12 H₂O, 0.15% H₂O₂, and 3.699 mM *o*-phenylenediamine) was added to each well. The reaction was allowed to proceed at 37°C for 15 min, and it was then stopped by addition of 50 μ l of 2 M H₂SO₄ to each well. The extent of enzyme activity was monitored by measuring absorbance at 490 nm with a microplate reader *Model 680* (Bio-Rad, CA, USA). Quantities of Rubisco subunits and the two activase isoforms were calculated according to the standard curves, plotted by parallel assays using serial concentration of purified Rubisco or expressed RCA fusion protein.

Plant material and growth conditions: Seeds of rice (*Oryza sativa* L. “Zhenong 952”) were germinated at 30°C and the germinated seeds were directly sown into the 15-l pot with 15 kg paddy soil until 3-leaf stage. Seedlings were thinned to 5 plants per pot and grown in a greenhouse with natural sunlight during the day at the Zijingang Campus of the Zhejiang University. The temperature was controlled about 30–35°C/20–25°C (day/night) and the relative humidity was maintained at 70%. When plants grew up to 9-leaf age (45 d after sowing), leaves from different positions were sampled at the same time of morning. All experiments were conducted using the middle part of each leaf from the main stem.

Measurement for gas exchange parameters and Rubisco activity: Measurements of gas exchange parameters were performed as described by Huang *et al.* (2004) using a portable photosynthesis system *LI-COR 6400* (*LI-COR Inc.*, Lincoln, NE, USA). The other conditions were controlled as follows: CO₂ concentration of $380 \pm 5 \mu\text{l dm}^{-3}$, photon flux density (PFD) of 1200 $\mu\text{mol}(\text{photon}) \text{m}^{-2} \text{s}^{-1}$, temperature of 30°C and relative humidity of 70%. After measurement of P_N , the leaf was immediately frozen in liquid nitrogen and stored at -80°C for measurement of Rubisco activity and Rubisco and RCA isoform contents. The results presented are the means \pm SD of 4–6 samples.

Rubisco initial and total activities were determined as described previously (Jin *et al.* 2006). Rubisco activation state was calculated as the relative ratio of initial to total Rubisco activities. Duplicate assays were conducted on each sample, each sample consisting of a leaf blade from a separate plant. The results presented are the means \pm SD of 4–6 samples.

Semiquantitative RT-PCR: Total RNA from each sample was extracted using the RNAiso Reagent (*TaKaRa*, Dalian, China) according to the manufacturer’s instructions. The concentration of total RNA was determined *via* optical density measurement using spectrophotometer *ND-1000* (*NanoDrop producer*, Delaware, USA). First strand cDNA was synthesized from 3 μg of total RNA using a *PrimeScript 1st Strand cDNA Synthesis Kit* (*TaKaRa*, Dalian, China, Japan) according to the supplier’s instructions. 2 μl cDNA was used as template for a 50 μl PCR reaction with rice actin primers and activase gene-specific primers. Actin was used as an internal standard (F 5'-TCCATCTTGGCATCTCTCAG-3'; R 5'-GTACCCGCATCAGGCATCTG-3'). As there is no specific sequence for specific PCR amplification of RCA_L mRNA (To *et al.* 1999), the RCA gene-specific primers (F 5'-CGTGACGGCGTATGGAGA-3'; R 5'-TTCCGGCACAGGCGGTTA-3') were designed for a region that includes the gene-specific region of RCAs mRNA. This results in an amplification product of 468 bp (denoting *rca_L* mRNA) and another amplification product of 550 bp (denoting *rca_S* mRNA). The PCR reaction was set up as follows: 94°C for 4 min; 25 cycles of 94°C for 30 s, 62°C for 30 s, 72°C for 1 min, followed by a final extension at 72°C for 10 min. Taq polymerase was purchased from *TaKaRa*, and the PCR mix was prepared according to the manufacturer’s instructions. The PCR products were checked with ethidium bromide-stained 2% (w/v) agarose gel in 1 \times TAE.

Results

Preparation of specific mAbs and establishment of ELISA for RCA isoforms and Rubisco subunits:

After inducing with IPTG, large amounts of His-tag fusion proteins were obtained. Result of SDS-PAGE showed that His-tag affinity purified pET-28a-COM or pET-32a-END fusion protein were consistent with the predicted molecular mass of 53 kDa (Fig. 2A, *lane 4*) or

30 kDa (Fig. 2B, *lane 4*) respectively. Western blot analysis indicated that the expressed His-tag fusion proteins not only reacted with anti-six-His antibody (Fig. 2A,B, *lane 5*), but also reacted specifically with rabbit anti-RCA serum (Fig. 2A,B, *lane 6*). These results demonstrated that the target proteins were successfully expressed.

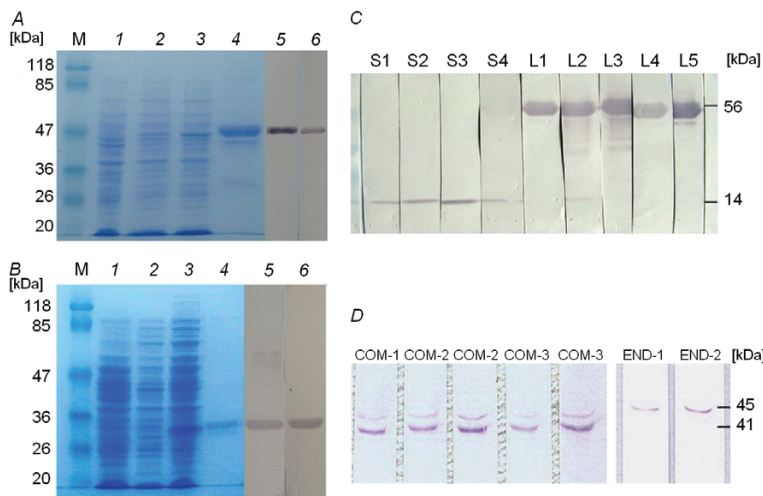


Fig. 2. Identification of fusion pET-28a-COM (A), pET-32a-END proteins (B) and monoclonal antibodies to Rubisco subunits (C) or RCA isoforms (D). A,B: Equal amount of lysates of recombinant bacteria (*lane 2*), IPTG induced recombinant bacteria (A,B: *lane 3*) and purified pET-28a-COM or pET-32a-END protein (A,B: *lane 4*) were separated by SDS-PAGE, while lysates of *E. coli* BL21 strain with pET-28a (A: *lane 1*) or pET-32a (B: *lane 1*) and protein marker (A,B: *lane M*) as controls. Purified pET-28a-COM and pET-32a-END protein were further transferred to a polyvinylidene fluoride membrane. Blots were probed with mAb to His tag (A,B: *lane 5*) and rabbit anti-RCA serum (A,B: *lane 6*) respectively, and visualized using alkaline phosphatase conjugated to a secondary antibody. C: monoclonal antibodies to Rubisco large subunit (C: L1 – L5) and monoclonal antibodies to Rubisco small subunit (C: S1 – S4). D: monoclonal antibodies to both RCA isoforms (D: COM-1 – COM-5) and monoclonal antibodies to RCA_L (D: END-1 – END-2). Antibodies were validated by Western blot analysis using natural total soluble proteins in rice leaf as an antigen. RCA – Rubisco activase.

Purified pET-28a-COM or pET-32a-END fusion protein and purified natural Rubisco subunit proteins were used as antigen to produce specific monoclonal antibodies (mAbs). The specificity of resulting mAbs was validated by Western blot analysis using natural RCA protein in rice leaf extract. As shown in Fig. 2C,D, there were five mAbs to RLS, four mAbs to RSS, five mAbs to pET-28a-COM protein reacting with both RCA_L and RCA_S, and two mAbs to pET-32a-END protein only recognizing RCA_L.

Based on the specific monoclonal antibodies to Rubisco subunits or RCA isoforms, series of enzyme-linked immunosorbent assays (ELISA) were established for quantitative analysis of Rubisco subunits and RCA isoforms. Linear range of antigen concentration and working dilutions of HRP-conjugated antibodies were determined by limited dilution assay (optimum parameters were shown in Table 1). Standard curves for RLS (Fig. 3A), RSS (Fig. 3B), total RCA (Fig. 3C) and RCA_L (Fig. 3D) were drawn in their linear ranges using

purified Rubisco subunits or immunopurified fusion proteins as standard samples, respectively. For quantitative analysis in leaf samples, leaf crude extracts were diluted for 1:640 for Rubisco subunits ELISA and diluted for 1:60 for RCA isoforms ELISA (Table 1). After quantifying RCA_L and total RCA content, the RCAs content could be calculated by subtraction.

Gas exchange parameters and Rubisco activity in different leaf positions: The results showed that P_N , transpiration rate (E) and stomatal conductance (g_s) changed with a similar pattern in different leaf positions (Fig. 4A,B,C). They reached the maximum in the fully developed leaf 8 and then declined gradually from leaf 7 to leaf 2 as their senescence. However, the intercellular CO_2 concentration (C) did not keep pace with the change of g_s , and it increased with leaf aging (Fig. 4D). This indicated that the stomatal limitation was not the key factor of decline of P_N during leaf aging.

Rubisco activity measurements showed that both

initial Rubisco activity and total Rubisco activity increased with leaf expanding and decreased with leaf aging (Fig. 5A,B). Interestingly, due to faster decline in initial Rubisco activity than total Rubisco activity, Rubisco activation state decreased with leaf aging (Fig. 5C). Regression analysis showed that P_N was most

significantly relative to initial Rubisco activity ($r = 0.945$, $P < 0.0001$), indicating that *in vivo* initial Rubisco activity played the most important role in determining P_N of leaf positions. Since initial Rubisco activity *in vivo* is maintained by RCA, it is necessary to determine the protein contents of Rubisco and RCA.

Table. 1 Characteristic parameters of direct ELISA

Parameters	RLS	RSS	RCA _L	Total RCA
Linear range of antigen concentration [$\mu\text{g cm}^{-3}$]	0.05–1.65	0.8–2.0	0.4–3.7	0.01–0.25
Working dilution of crude extract before coating	1:640	1:640	1:60	1:60
Working dilution of HRP-conjugated antibody	1:8000	1:6000	1:2000	1:4000

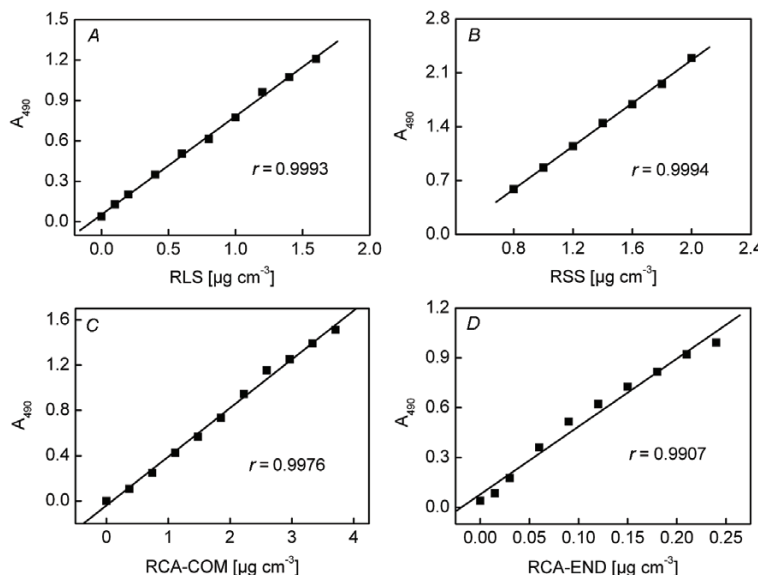


Fig. 3. Standard curves for developed direct ELISA. A: standard curve for Rubisco large subunit (RLS); B: standard curve for Rubisco small subunit (RSS); C: standard curve for total Rubisco activase (RCA); D: standard curve for RCA large isoform (RCA_L). Standard curves were drawn in their linear range.

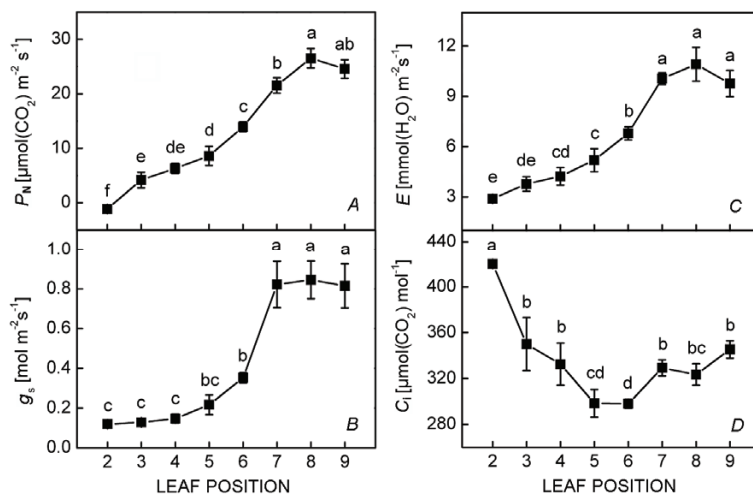


Fig. 4. Gas exchange parameters in different leaf positions. P_N (A), E (B), g_s (C) and C_i (D) of leaves were measured at PFD of $1200 \mu\text{mol m}^{-2} \text{s}^{-1}$, CO_2 concentration of $380 \pm 5 \mu\text{l dm}^{-3}$, temperature of 30°C and relative humidity of 70%. Symbols marked with the same letters were not significantly different ($P < 0.05$) for different samples. The results presented are the means $\pm \text{SD}$ ($n=4$).

Contents of Rubisco subunits and RCA isoforms in different leaf positions: The ELISA assays were further employed for rapid determination of Rubisco subunits content and two RCA isoforms content in different leaf positions. As shown in Fig. 6A,B, both amount of RLS and RSS reached the maximum in fully expanded new leaf (leaf 8). The youngest leaf in the top (leaf 9) exhibited less RLS and RSS accumulation than the 8th one. With leaf aging from the 7th to 2nd leaf, both amount of RLS and RSS declined gradually. However, molar ratio of RLS versus RSS maintained a relatively steady value of 0.95–1.07 in all leaves (Fig. 6C), indicating that expression of RLS and RSS were coordinated during leaf development. Unlike the balance of two Rubisco subunits, the accumulation of RCA_S (Fig. 6E) was at least 5-fold more than that of RCA_L (Fig. 6D) in all leaves. In addition, with the decline of both RCA_L and RCA_S content during leaf aging the molar ratio of RCA_L versus RCA_S decreased from 0.194 in the 8th leaf to 0.014 in the

2nd leaf (Fig. 6F), suggesting that the decline of RCA_L accumulation was more pronounced than that of RCA_S. Further analysis showed that there was extremely significant linear relationship between Rubisco activation state and RCA_L/RCA_S ratio ($r = 0.935, P < 0.0001$), means the RCA_L/RCA_S ratio might play an important role in regulation of Rubisco activation and P_N during leaf aging.

mRNA accumulation of two RCA isoforms in different leaf positions: In order to examine if the change in ratio of two RCA isoforms in different leaf positions was attributed to transcriptional regulation, mRNA accumulation of two RCA isoforms was determined. The results of RT-PCR showed a relatively steady ratio (~ 0.15) of *rca-L/rca-S*, although the total mRNA accumulation decreased with leaf aging (Fig. 7), suggesting that the change of RCA isoforms ratio in different leaf positions was not caused by transcriptional regulation.

Discussion

Quantitive analysis of RCA isoforms by ELISA: Quantitive analysis of RCA isoform contents reported in the literature is mainly conducted by the method of Westernblot. Although this is an effective method for quantitive analysis of specific protein, it is not convenient for a great number of samples. In this work, a set of ELISA based on highly specific mAbs were developed for accurately quantitive analysis of RCA isoforms as well as Rubisco subunits. This is the first set of method using ELISA to assay the different RCA isoforms and the first report on contents of RCA isoforms in different leaf positions. Our results showed a RCA_L/RCA_S ratio of 1:5 in fully expanded rice leaves (Fig. 6F). It has been reported that the RCA_L is susceptible to proteolytic degradation (Zielinski *et al.* 1989). To test whether the relative low proportion of RCA_L was caused by its degradation during ELISA, Westernblot of leaf extracts from spinach and rice was probed with rice mAbs against the common section of two RCA polypeptides (Fig. 8). The result showed that spinach contained two isoforms with almost equal amount as reported by other study (Salvucci *et al.* 1987), while rice contained two isoforms with more amount of small isoform in consistence with the result of ELISA. This demonstrated that the relatively low amount of RCA_L in rice was not mainly due to its proteolytic degradation. Two significantly different RCA_L/RCA_S ratios in rice leaves have been reported by the method of Westernblot (To *et al.* 1999, Wu *et al.* 2007), but our observation is more consistent with the result reported by To *et al.* (1999). Analysis for *rca* mRNA accumulation further indicated that the low RCA_L/RCA_S ratio resulted from difference in their mRNA levels in rice leaf (Fig. 7). These results suggest that the alternative splicing of *rca* pre-mRNA in rice prefers to produce relatively more amount of RCA_S isoform.

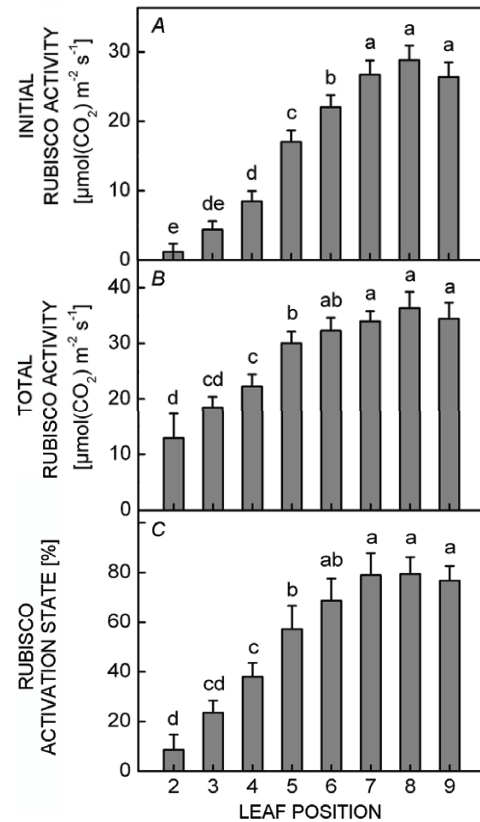


Fig. 5. Rubisco activity in different leaf positions. Initial Rubisco activity (A) and total Rubisco activity (B) of each sample were determined after gas exchange measurements. Rubisco activation state was calculated as the relative ratio of initial to total Rubisco activities. Symbols marked with the same letters were not significantly different ($P < 0.05$) for different samples. The results presented are the means \pm SD ($n = 4$).

The change of RCA_L/RCA_S in different leaf position not due to transcriptional regulation: The coordinate expression of Rubisco and total RCA during leaf development has been studied early (Zielinski *et al.* 1989), but the detail in expression of two different RCA isoforms which are encoded by one gene is rarely reported. Our results showed that the molar ratio of RCA_L versus RCA_S increased with leaf expanding and decreased significantly during leaf aging (Fig. 6F), although both amount of Rubisco subunits (RLS and RSS) and RCA isoforms changed with leaf positions (Fig. 6A,B,D,E). Analysis of mRNA accumulation further revealed that there was no obvious change in the ratio of two RCA isoform mRNA accumulation in different leaf positions (Fig. 7), suggesting that the change in molar ratio of two RCA polypeptides was not caused by transcriptional regulation. It is well known that the

content of proteinases and growth inhibitors increases with leaf senescence, which accelerates the proteo metabolism and amino acid transfer from aging leaves to young ones (Thimann 1982), and the senescence-associated events mostly happen in translational level rather than in the transcriptional one (Thomas and Stoddart 1982). Furthermore, the C-extension of RCA_L is reported to be susceptible to proteolytic degradation (Zielinski *et al.* 1989). Hence, it is likely that the altered RCA_L/RCA_S ratio during leaf aging was associated with post-translational modification of RCA_L .

The relationship between RCA isoforms and P_N : During leaf aging, decreased g_s and increased C_i suggested that the decline of P_N was mainly attributed to the nonstomatal limitation (Farquhar and Sharkey 1982). Senescence-correlated losses in photosynthetic capacity

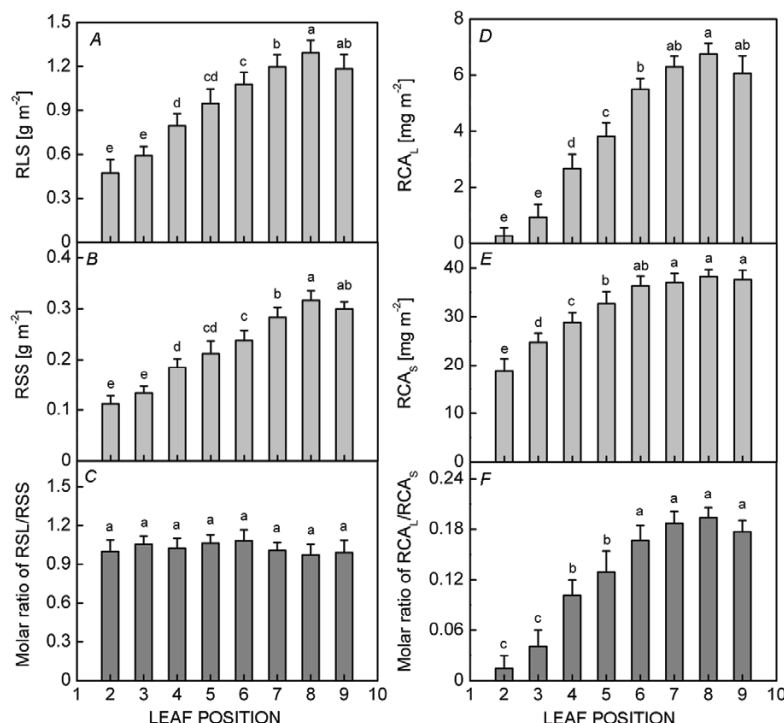


Fig. 6. The accumulations of Rubisco large subunit (RLS) (A), Rubisco small subunit (RSS) (B), RCA large isoform (RCA_L) (D) and RCA small isoform (RCA_S) (E) in different leaf positions (2nd–9th leaf). Molar ratio of RLS/RSS (C) and molar ratio of RCA_L/RCA_S (F) in different leaf positions were calculated based on protein content. Symbols marked with the same letters were not significantly different ($P<0.05$) for different samples.

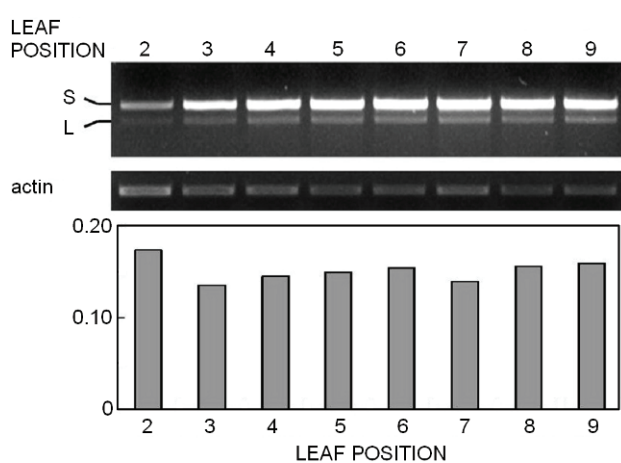


Fig. 7. Accumulation of *rca* mRNA in different leaf positions. Total RNA from each sample was extracted as described in Materials and methods. RT-PCR analysis was performed with actin as a control. Amplification products of the *rca_L* (L) and the *rca_S* (S) mRNA were presented in a 2% agarose gel. The densitometric analysis of bands was performed with quantity one software, and the calculated ratio of *rca_L/rca_S* were shown (bottom).

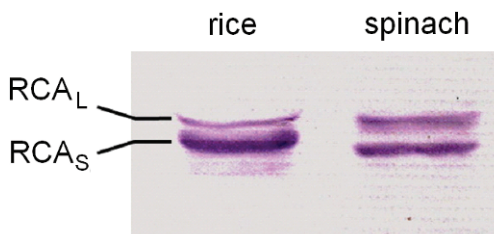


Fig. 8. Rubisco activase (RCA) isoforms from rice (*left lane*) and spinach (*right lane*). Extracts of total soluble protein from rice and spinach fully expanded young leaves were separated by SDS-PAGE and transferred to a PVDF membrane. Blots were probed with antibodies to RCA and visualized using alkaline phosphatase conjugated to a secondary antibody.

are usually associated with alterations in Rubisco activity, which may arise as a consequence of changes in either amount and/or activation of the enzyme (Gepstein 1988). Our results showed that the changes in amount of both Rubisco and RCA protein (Fig. 6) paralleled the changes in P_N (Fig. 4A), which indicated that the decreased photosynthetic capacity during leaf aging might be attributed to the loss of Rubisco. In fact, only activated Rubisco *in vivo* can catalyze CO_2 fixation. Hence, the initial activity should play more important role in the regulation of photosynthesis. Our results showed that the leaf with the highest P_N exhibited the highest initial Rubisco activity and Rubisco activation state (Figs. 4A, 5A,C). Jiang and Xu (1995) reported that P_N is most correlative to initial Rubisco activity during leaf senescence. Our results also showed that the highest linear correlation occurred between P_N and initial Rubisco activity.

References

Demirevska-Kepova, K., Kandiisky, D., Juperlieva-Mateeva, B.: Quantitative determination of ribulose-1,5-bisphosphate carboxylase/oxygenase in leaf extracts from barley plants by enzyme-linked immunosorbent assay. – *Trends biochem. Sci.* **24**: 637-640, 1990.

Farquhar, G.D., Sharkey, T.D.: Stomatal conductance and photosynthesis. – *Annu. Rev. Plant Physiol.* **33**: 317-345, 1982.

Gepstein, S.: Photosynthesis. – In: Noodén, L.D., Leopold, A.C. (ed.): *Senescence and Aging in Plants*. Pp. 85-109. Academic Press, San Diego – New York – Berkeley – Boston – London – Sydney – Tokyo – Toronto 1988.

Huang, Z.-A., Jiang, D.-A., Yang, Y., Sun, J.-W., Jin, S.-H.: Effects of nitrogen deficiency on gas exchange, chlorophyll fluorescence and antioxidant enzymes in leaf rice plants. – *Photosynthetica* **42**: 357-364, 2004.

Lilley, R.M., Portis, A.R., Jr.: ATP hydrolysis activity and polymerization state of ribulose-1,5-bisphosphate carboxylase oxygenase activase - Do the effects of Mg^{2+} , K^+ , and activase concentrations indicate a functional similarity to actin? – *Plant Physiol.* **114**: 605-613, 1997.

Lu, K.X., Yang Y., He, Y., Jiang, D.A.: Induction of cyclic electron flow around photosystem 1 and state transition are correlated with salt tolerance in soybean. – *Photosynthetica* **46**: 10-16, 2008.

Jiang, D.A., Xu, Y.F.: Internal dominant factors for declination of photosynthesis during rice leaf senescence. – *J. Zhejiang Agri. Univ.* **21**: 533-538, 1995.

Jin, S.H., Hong, J., Li, X.-Q., Jiang, D.-A.: Antisense inhibition of Rubisco activase increases Rubisco content and alters the proportion of Rubisco activase in stroma and thylakoids in chloroplasts of rice leaves. – *Ann. Bot.* **97**: 736-744, 2006.

Makino, A., Mae, T., Ohira, K.: Purification and storage of ribulose 1,5-bisphosphate carboxylase from rice leaves. – *Plant Cell Physiol.* **24**: 1169-1173, 1983.

Portis, A.R., Jr.: Rubisco activase. – *Biochim. Biophys. Acta* **1015**: 15-28, 1990.

Portis, A.R., Jr.: Regulation of ribulose 1,5-bisphosphate carboxylase oxygenase activity. – *Annu. Rev. Plant Physiol. Plant Mol. Biol.* **43**: 415-437, 1992.

Portis, A.R., Jr.: Rubisco activase-Rubisco's catalytic chaperone. – *Photosynth. Res.* **75**: 11-27, 2003.

Rundle, S.J., Zielinski, R.E.: Alterations in barley ribulose-1,5-bisphosphate carboxylase oxygenase activase gene-expression during development and in response to illumination. – *J. Biol. Chem.* **266**: 14802-14807, 1991.

Salvucci, M.E., Ogren, W.L.: The mechanism of Rubisco

activase: Insights from studies of the properties and structure of the enzyme. – *Photosynth. Res.* **47**: 1-11, 1996.

Salvucci, M.E., Werneke, J.M., Ogren, W.L., Portis, A.R., Jr.: Purification and species distribution of Rubisco activase. – *Plant Physiol.* **84**: 930-936, 1987.

Shen, J.B., Orozco, E.M., Ogren, W.L.: Expression of the 2 isoforms of spinach ribulose 1,5-bisphosphate carboxylase activase and essentiality of the conserved lysine in the consensus nucleotide-binding domain. – *J. Biol. Chem.* **266**: 8963-8968, 1991.

Streusand, V.J., Portis, A.R., Jr.: Rubisco activase mediates ATP-dependent activation of ribulosebisphosphate carboxylase. – *Plant Physiol.* **85**: 152-154, 1987.

Thimann, K.V.: The senescence of leaves. – In: Thimann, K.V. (ed.): *Senescence in Plants*. Pp. 85-115. CRC Press, Boca Raton, 1982.

Thomas, H., Stoddart, J.L.: Leaf senescence. – *Annu. Rev. Plant Physiol.* **31**: 83-111, 1982.

To, K.-Y., Suen, D.-F., Chen, S.-C. G.: Molecular characterization of ribulose-1,5-bisphosphate carboxylase/oxygenase in rice leaves. – *Planta* **209**: 66-76, 1999.

Vargas-Suárez, M., Ayala-Ochoa, A., Lozano-Franco, J., García-Torres, I., Díaz-Quiñonez, A., Ortíz-Navarrete, V.F., Sánchez-de-Jiménez, E.: Rubisco activase chaperone activity is regulated by a post-translational mechanism in maize leaves. – *J. Exp. Bot.* **55**: 2533-2539, 2004.

Wang, D.F., Portis, A.R., Jr.: Increased sensitivity of oxidized large isoform of ribulose-1,5-bisphosphate carboxylase/oxygenase (Rubisco) activase to ADP inhibition is due to an interaction between its carboxyl extension and nucleotide-binding pocket. – *J. Biol. Chem.* **281**: 25241-25249, 2006.

Werneke, J.M., Chatfield, J.M., Ogren, W.L.: Alternative messenger-RNA splicing generates the 2 ribulose bisphosphate carboxylase/oxygenase polypeptides in spinach and *Arabidopsis*. – *Plant Cell* **1**: 815-825, 1989.

Wilson, M., Nakane, P.K.: *Immunofluorescence and Related Staining Techniques*. – Elsevier/North Holland Biomedical Press, Amsterdam 1978.

Wu, H.R., Li, L.B., Jing, Y.X., Kuang, T.Y.: Over- and anti-sense expressions of the large isoform of ribulose-1,5-bisphosphate carboxylase/oxygenase activase gene in *Oryza sativa* affect the photosynthetic capacity. – *Photosynthetica* **45**: 194-201, 2007.

Zhang, N., Kallis, R.P., Ewy, R.G., Portis, A.R., Jr.: Light modulation of Rubisco in *Arabidopsis* requires a capacity for redox regulation of the larger Rubisco activase isoform. – *Proc. Nat. Acad. Sci. USA* **99**: 3330-3334, 2002.

Zhang, N., Schürmann, P., Portis, A.R., Jr.: Characterization of the regulatory function of the 46-kDa isoform of Rubisco activase from *Arabidopsis*. – *Photosynth. Res.* **68**: 29-37, 2001.

Zhang, N., Portis, A.R., Jr.: Mechanism of light regulation of Rubisco: A specific role for the larger Rubisco activase isoform involving reductive activation by thioredoxin-f. – *Proc. Nat. Acad. Sci. USA* **96**: 9438-9443, 1999.

Zhang, Z.L., Komatsu, S.: Molecular cloning and characterization of cDNAs encoding two isoforms of ribulose-1,5-bisphosphate carboxylase/oxygenase activase in rice (*Oryza sativa* L.). – *J. Biochem.* **128**: 383-389, 2000.

Zhou, J.Y., Shang, S.B., Gong, H., Chen, Q.X., Wu, J.X., Shen, H.G., Chen, T.F., Guo, J.Q.: In vitro expression, monoclonal antibody and bioactivity for capsid protein of porcine circovirus type II without nuclear localization signal. – *J. Biotechnology* **118**: 201-211, 2005.

Zielinski, R.E., Werneke, J.M., Jenkins, M.E.: Coordinate expression of Rubisco activase and Rubisco during barley leaf cell-development. – *Plant Physiol.* **90**: 516-521, 1989.